HHS Public Access

Author manuscript

J Orthop Res. Author manuscript; available in PMC 2019 October 01.

Published in final edited form as:

J Orthop Res. 2018 October ; 36(10): 2622–2632. doi:10.1002/jor.24027.

Knockout of Hyaluronan Synthase 1, but not 3, Impairs Formation of the Retrocalcaneal Bursa

Katie J. Sikes[1,2], **Kristen Renner**[3], **Jun Li**[4], **K. Jane Grande-Allen**[5], **Jennifer P. Connell**[5], **Valbona Cali**[6], **Ronald J. Midura**[6], **John D. Sandy**[1], **Anna Plaas**[1,4,*], and **Vincent M. Wang**[2,3]

[1]Department of Orthopedic Surgery, Rush University Medical Center, 1611 W. Harrison Street, Chicago, IL 60612

[2]Department of Bioengineering, University of Illinois at Chicago, 851 S. Morgan Street, Chicago, IL 60607

[3]Department of Biomedical Engineering and Mechanics, Virginia Tech, 339 Kelly Hall, 325 Stanger Street MC 0298, Blacksburg, VA, 24061

[4]Department of Internal Medicine (Rheumatology), Rush University Medical Center, 1611 W. Harrison Street, Chicago, IL 60612

[5]Department of Bioengineering, Rice University, 6100 Main Street, Houston, TX 77005

[6]Lerner Research Institute, The Cleveland Clinic Foundation, 9500 Euclid Avenue Cleveland, OH 44195

Abstract

Hyaluronan (HA), a high molecular weight non-sulfated glycosaminoglycan, is an integral component of the extracellular matrix of developing and mature connective tissues including tendon. There are few published reports quantifying HA content during tendon growth and maturation, or detailing its effects on the mechanical properties of the tendon extracellular matrix. Therefore, the goal of the current study was to examine the role of HA synthesis during post-natal skeletal growth and maturation, and its influence on tendon structure and biomechanical function. For this purpose, the morphological, biochemical, and mechanical properties of Achilles tendons from wild type (WT) and hyaluronan synthase 1 and 3 deficient mouse strains (*Has1*$^{-/-}$ (Has1KO), *Has3*$^{-/-}$ (Has3KO), and *Has1*$^{-/-}$*3*$^{-/-}$ (Has1/3KO)) were determined at 4, 8, and 12 weeks of age. Overall, HAS-deficient mice did not show any marked differences from WT mice in Achilles

*Corresponding Author Anna Plaas, PhD, Rush University Medical Center, 1611 W Harrison Street Suite 510, Chicago, IL 60612, Phone: (312) 498-4970, Fax: (312) 563-2267, anna_plaas@rush.edu.

Author Contribution statements:

All authors have read and approved the final submitted manuscript

Sikes, Katie J – Animal work, Biomechanical testing, qt-PCR, Manuscript Preparation

Renner, Kristen – Biomechanical Testing

Li, Jun – Animal work, Histology

Grande-Allen, Jane – Picrosirius Red Staining and Analysis

Connell, Jennifer P – Picrosirius Red Staining and Analysis

Cali, Valbona – FACE analysis

Midura, Ronald J – FACE analysis

Sandy, John D – Experimental Design, Manuscript Preparation

Plaas, A – Experimental Design, Histological Imaging, Manuscript Preparation

Wang, Vincent M – Experimental Design, Biomechanical Testing, Manuscript Preparation

tendon morphology or in the HA and chondroitin/dermatan sulfate (CS/DS) contents. However, *HAS1*-deficiency (in the single or Has1/3 double KO) impeded post-natal formation of the retrocalcaneal bursa, implicating HAS1 in regulating HA metabolism by cells lining the bursal cavity. Together, these data suggest that HA metabolism via HAS1 and HAS3 does not markedly influence the extracellular matrix structure or function of the tendon body, but plays a role in the formation/maintenance of peritendinous bursa. Additional studies are warranted to elucidate the relationship of HA and CS/DS metabolism to tendon healing and repair *in-vivo*.

Keywords

Hyaluronan; Hyaluronan Synthases; Tendon; Bursa; Collagen

Introduction

Hyaluronan (HA), a high molecular weight non-sulfated glycosaminoglycan (GAG), is an integral component of the extracellular matrix (ECM) of developing and mature connective tissues. At the molecular level, a metastable homeostatic interaction between HA and H_2O molecules can form to promote tissue hydration and surface lubrication (1–3). From a biophysical perspective, the size, hydration, and hydrodynamic shape of HA polymers provide for high viscosity and increased relaxation time, thereby conferring viscoelasticity during physical deformation (4).

While HA is synthesized as a core-protein-free GAG, it is immobilized by cell surface receptors (5) such as CD44, LYVE, RHAMM, or TLRs, or assembles within the ECM into networks in association with a variety of specific binding proteins (HABPs) (6). The interactions of these various HABPs with HA results in distinct mechanical and metabolic functionalities (7). For example, aggrecan and versican, together with link protein, bind to HA to form large complexes which contribute to the structural integrity of cartilage and blood vessels (2). In response to inflammatory stimuli, Tumor Necrosis Factor Stimulated Gene-6 (TSG-6) and Pentraxin 3 mediate a cross-linking interaction between HA and Heavy Chains which regulate downstream inflammatory processes (8).

HA is synthesized by transmembrane hyaluronan synthases (HASs) (9). To date, three isoforms have been identified, HAS1, HAS2, and HAS3, and their functional activity is regulated transcriptionally (10–13), by post-translational modification (10, 14), and via transport to the plasma membrane from the Golgi (HAS1 and HAS3) or the endoplasmic reticulum (HAS2) (10). Specific *in-vitro* catalytic properties (e.g., Km values and the chain length generated) distinguish the isoforms (9, 10, 15), and spatial and temporal expression of the three isoforms during embryonic development has been reported. Specific HAS isoform expressions have been implicated in tooth (16) and cardiac (17–19) development, with HAS2 (17) linked to atrioventricular valve morphology and cardiac left-right asymmetry. Additionally, HAS2 expression appears to spatially complement that of *HAS3*, specifically with regard to sensory development. HAS1 expression complements HAS2 during early development (20). Moreover, HAS1-deficient mice exhibit aberrant dermal wound healing and excessive fibrotic remodeling of the joint capsule (21, 22), but the *in-vivo* functions of

HAS1 and HAS3 during skeletal development and growth remain largely unknown. Indeed, recent evidence highlights the role of HAS isoforms in accessory functions other than HA synthesis (10), with cross-talk between the isoforms representing a relatively un-explored niche.

The contribution of endogenous HA to tendon structure and biomechanical function is poorly understood. To date, there are very few published reports quantifying HA content during tendon growth and maturation, nor detailing the possible effect on the mechanical properties of the tendon ECM. Early studies demonstrated that both the dermatan sulfate (DS) and HA contents of rat tail tendons decreased during maturation (23). Additionally, murine studies with gene-deletions have characterized the influence of chondroitin/dermatan sulfate (CS/DS) and keratan sulfate substituted small leucine rich proteoglycans (SLRPs) on tendon ultrastructural and mechanical properties at various stages of growth and development (24–30). Their absence leads to the formation of irregularly-shaped collagen fibrils and altered fibril diameter distributions with age and tendon-specific alterations in tissue mechanical properties. In the context of the *in-vivo* function of the Achilles-calcaneus complex, it is important to note that in addition to the tendon body, HA is a component of the tendon-bone insertion, and it is secreted into the retrocaneal bursa by the surrounding lining cells.

The goal of the current study was to examine the role of HA synthases in post-natal maturation and biomechanical function of the Achilles-calcaneus complex. Given the role of HAS isoforms in accessory functions such as inflammation (21, 31, 32) and wound healing (10), we hypothesized that HAS1 and HAS3 exhibit unique non-redundant effects on tendon structure and function. We report here on the morphological characteristics of the Achilles-calcaneus complex, as well as the gene expression, biochemical, and mechanical properties of the tendon in C57Bl6 wild type and hyaluronan synthase 1 and 3 deficient mouse strains, (Has1KO), (Has3KO), and (Has1/3KO) at 4, 8, and 12 weeks of age.

Materials and Methods

Animals

All animal use was approved by the Rush University IACUC. Wild-type (WT), Has1KO, Has3KO, and Has1/3KO mice were bred in-house as previously described (21). Of note, investigation of *Has2* knockout in the present study design was not feasible since constitutive knockout of this gene is lethal in mice (33). A total of 248 mice were used for this study, with 107, 82, and 125 mice used for 4, 8, and 12 week old time-points, respectively. Experimental groups and outcomes are summarized in Table 1. At weaning, male pups were separated and distributed randomly into the experimental groups, with n=6 animals per cage. Mice had free access to water and chow, and were exposed to the same light cycles (12 hour light, 12 hour dark) during the growth period. Mice were sacrificed at 4, 8, or 12 weeks of age by CO_2 asphyxiation and cervical dislocation. Within 15 minutes of sacrifice, Achilles tendons from both limbs were isolated from all surrounding tissues with the peritenon left intact and immediately placed into proteinase K or RNALater solutions, and processed for FACE or gene expression analysis, respectively, as described below. For histology, both legs were dissected of all skin and placed in formalin for at least 1 day,

followed by decalcification in EDTA for 2 weeks, as previously described (34, 35). For biomechanical testing, carcasses were frozen at −20°C until the day of testing.

Histology and Picrosirius Red Staining

Specimens were formalin fixed, decalcified, processed, embedded in paraffin, and 5 μm thin sagittal sections were cut through the entire ankle joint. For histopathology, sections were stained with Safranin O and Fast-Green counterstain. This stain was used to assess potential aggrecan deposits in tendons of the KO mice and to assess the appearance of fibrocartilaginous region at the tendon/calcaneous insertion site (Figure 2). For HA staining, sections were deparaffinized, and incubated overnight at 4°C for hyaluronan which was localized using a biotinylated HA Binding Protein (bHrTSG6) under a MTA from Halozyme (San Diego, CA).

To assess collagen alignment, tissue sections were rehydrated and stained with picrosirius red solution (PRS) of 0.1% w/v sirius red F3B (Direct Red 80, Sigma-Aldrich, St. Louis, MO) in saturated aqueous solution of picric acid (Sigma Aldrich) for 1 hour. Sections were then rinsed with acidified water (1% acetic acid), dehydrated, mounted, and visualized under polarized light to capture maximal birefringence. Note that larger, highly aligned, densely packed collagen fibers are red or orange under polarized light (longer wavelengths) while smaller collagen fibers are green, with the absence of color in an area indicative of the absence of aligned collagen fibers (36, 37).

Fluorophore Assisted Carbohydrate Analyses (FACE)

The content of HA and chondroitin sulfate/dermatan sulfate (CS/DS) in Achilles tendons was quantified as previously described (38). For each experimental group (Table 1), two or four pools of 5–8 Achilles tendons each were digested with 100–150 uL of Proteinase K (PK) at 55°C for 18 hours prior to isolation of GAGs, chondroitinase ABC digestion, fluorotagging, and electrophoretic separation of ΔdiHA, Δdi0S, Δdi6S and Δdi4S (38–40). Contents were normalized to the digest volume followed by normalization to the tendon geometric volume (total number of tendons in the digest X average tendon volume, as measured from the samples undergoing biomechanical testing). Statistical significance between age-matched genotypes was determined using a one-way ANOVA with Tukey's post-hoc tests ($p<0.05$) in GraphPad Prism 7. For genotype matched age comparisons between groups with more than 2 replicate pools (4 vs. 12 week age groups only), a Student's t-test ($p<0.05$) was used.

Gene Expression

RNA was isolated from tissue pools each containing 10–24 individual tendons (Table 1), as previously described (34, 35). While RNA yields were similar among the four genotypes, yields varied by age (~1040 ng/tendon at 4 weeks, ~540 ng/tendon at 8 weeks, and ~220 ng/tendon at 12 weeks of age). cDNA was synthesized with 0.5ug of mRNA (A260:A280>1.90) using the RT^2 First Strand Kit (Qiagen) and transcript abundances were determined via qt-PCR using Taqman primers from Life Technologies (Carlsbad, CA) for the following genes: *Glyceraldehyde-3-phosphate dehydrogenase (Gapdh*, (Mm99999915_g1), *Collagen Type I alpha 1* (*Col1a1*, Mm00801666_g1), *Collagen Type III alpha 1* (*Col3a1*, Mm00802331_m1),

Decorin (Dcn, Mm00514535), *Biglycan* (*Bgn,* Mm01191753), *Fibromodulin, (Fmod,* mM00491215), *Hyaluronan Synthase 1 (Has1,* Mm00468496_m1), *Hyaluronan Synthase 2 (Has,* Mm00515089_m1), and for *Hyaluronan Synthase 3* (*Has3*, Mm00515092_m1). ΔCt values (Ct *gene of interest* minus Ct for *Gapdh*) were used to calculate an apparent transcript abundance (2^-(ΔCt)*1000) with arbitrary units. Additionally, the fold change in HAS-deficient genotypes relative to WT was calculated as 2^- ΔΔCt, with ΔΔCt calculated from ΔCt of HAS-deficient genotype minus ΔCt of WT. *Has3* and *Col2a1* transcripts were not detected (Ct>34) in any experimental group.

Statistical comparisons between groups with n=3 pools (WT, Has1KO, and Has3KO at 4 and 12 weeks of age only, see Table 1) was conducted in GraphPad Prism 7. Specifically, comparisons among age-matched genotypes was determined using a one-way ANOVA with Tukey's post-hoc tests ($p<0.05$). For genotype-matched age comparisons, a Student's t-test ($p<0.05$) was used. Overall, pooling of 10–24 tendons per group ensured high yields of pure RNA (see Supplemental Table 1), for the assay of multiple genes. The Ct expression values of *Gapdh* and *Col1a1* across our studies utilizing 12 week old WT murine Achilles tendons demonstrates the reproducibility of our expression assays (34, 35).

Biomechanical Testing

The Achilles-calcaneus complex was dissected from all surrounding tissue. Width and length were measured for each tendon using precision calipers and thickness was measured using a laser displacement sensor (Model #LK-G82, Keyence, Itasca, IL), as previously described (38). These dimensions were recorded at three locations along the tendon length, and cross-sectional area (CSA) was calculated as the product of the average width and thickness. Volume (used to normalize GAG content measurements, as detailed below) was calculated as the product of the CSA and tendon length. The calcaneus was potted in dental cement (Stoelting Co., Wood Dale, IL) and the tendon-bone construct was oriented at 45° plantar flexion using custom fixtures. All tensile testing was conducted in a room temperature isotonic saline bath. The following protocol was utilized for each specimen: preload to establish initial tendon length, preconditioning (20 cycles), 15-minute stress-relaxation test at 5% grip-to-grip strain, and load-to-failure at 0.05 mm/sec. Due to differences in tendon size across the age groups for 4, 8, and 12 week tendons, clamped (un-loaded) tendon lengths were 4mm, 5mm, and 6mm; pre-load magnitudes were 0.01N, 0.02N, and 0.05N, while preconditioning load endpoints were 0.01–0.08N, 0.05–0.15N, and 0.05–0.55N, respectively.

From stress relaxation testing, the following parameters were calculated: percent relaxation (determined as $\frac{\sigma_p - \sigma_e}{\sigma_p}$ where σ_p is peak stress and σ_e is equilibrium stress), and the Quasi-Linear Viscoelastic (QLV) mathematical modeling parameters A, B, C, Tau1, and Tau2 determined by curve-fitting the experimental data. QLV theory has been shown to accurately model the stress-relaxation behavior of ligaments and tendons (41, 42) using test protocols closely resembling that of the present study. QLV coefficients describe the non-linear elastic behavior (elastic stress constant A and elastic power constant B) as well as the viscous

components (relaxation index C, and short and long relaxation time constants Tau1, and Tau2, respectively) of the material (43).

From load-to-failure testing, structural properties including maximum force, extension at maximum force, stiffness, and work to maximum force were determined. Additionally, material properties (maximum stress, strain at maximum stress, elastic modulus, and energy to maximum stress) were calculated by normalizing the load and displacement values by the CSA and initial length (38). Separate 1-way ANOVAs were used to compare the four genotypes at each age as well as to examine age-dependent differences within each genotype. When the independent factors (age or genotype) revealed a significant difference ($p<0.05$), Tukey's post–hoc comparisons were used to determine pairwise differences among levels within each factor. All statistical tests were conducted in GraphPad Prism 7 (La Jolla, CA) ($p<0.05$).

Results

The Effect of HAS Deficiency on Tendon Morphology and HA Concentrations

SafraninO stained sections of the Achilles tendon body showed no marked differences between genotypes with regard to collagen organization, cell density, or overall morphology (Figure 1A). Additionally, localization studies (Figure 1A), showed no marked differences in intra-tendinous HA staining between genotypes at any age. Also, no significant ($p>0.05$) difference in tendon HA concentration (approximately 0.015–0.025 μg/μl), relative to tendon volume (mm^3), was detected between the genotypes at 4 and 12 weeks of age (Figure 1B), and age-dependent changes were not detected for any genotype. Notably, the range of values was markedly greater at 4 weeks in all genotypes relative to 8 and 12 weeks, possibly due to variability in tendon growth at 4 weeks due to pre-weaning (litter size and feeding success) and/or post-weaning (ease of climbing to access food and water) variables. Notably, no significant differences in HAS isoform expression was detected in WT (*Has1*: p=0.79, *Has2*: p=0.32), Has1KO (*Has2*: p=0.78), or Has3KO (*Has1*: p=0.51, Has2: p=0.40) tendons with age (Table 2). Additionally, age-matched genotype comparisons of *Has2* expression yielded no significant differences (4 weeks: p=0.19, 12 weeks: p=0.99, Table 2).

The Effect of HAS Deficiency on Formation of the Retrocalcaneal Bursa

HAS1-deficiency (in the single or Has1/3 double KO) at all ages was accompanied by a failure to develop an HA-rich fluid-filled retro-calcaneal bursa (Figure 2). Instead, this bursal space was filled with a cell-rich fibrous ingrowth extending from the proximal Kager's fat pad, which stained strongly for the presence of HA at all ages. For both HAS1-positive genotypes (WT and Has3KO) at 8 and 12 weeks, the bursal space was filled with a lightly-stained and largely cell-free matrix, consistent with a typical HA-containing fluid-filled bursa.

The Effect of HAS Deficiency on Collagen Organization and Expression in Achilles Tendons

Picrosirius red (PSR) staining showed minor apparent differences at 4 weeks of age in the four genotypes examined (Figure 3). Primarily, the collagen fibers appeared less organized

with single HAS1-deficiency (Has1KO) throughout the tendon body, and at the insertion site (**white arrows,** Figure 3), but these differences were not evident with SafO staining (Figure 1A). Conversely, HAS3-deficiency (Has3KO and Has1/3KO) appeared to result in more densely packed fibers in the distal tendon body (**black arrows,** Figure 3). By 12 weeks of age, no differences in PSR outcomes were detected between the genotypes suggesting a more highly organized ECM with the completion of growth of all genotypes (Figure 3). With respect to collagen expression, HAS1-deficiency only (Has1KO) resulted in reduced expression of *Col3a1* relative to WT at 12 weeks of age (−13.54-fold, p=0.003, Table 3). No other significant differences in *Col1a1* and *Col3a1* expression in HAS-deficient genotypes relative to age-matched WT were detected. Notably, with maturation, a significant reduction in *Col1a1* and *Col3a1* was evident in both WT (*Col1a1*: p=0.002, *Col3a1*: p=0.02) and Has1KO (*Col1a1*: p=0.01, *Col3a1:* p=0.008) genotypes, and *Col3a1* was significantly (p=0.04) reduced in Has3KO mice.

The Effect of HAS Deficiency on CS/DS contents in Achilles Tendons

As observed for HA, the concentration of CS/DS relative to tendon volume (mm^3), was markedly variable at 4 weeks compared to 8 and 12 weeks in all genotypes (Figure 4), consistent with the expected differences between individual mice in the rapid growth phase. No significant differences in CS/DS contents were detected from age-matched genotypic comparisons (4 weeks: p=0.98, 12 weeks: p=0.86). Genotype-matched comparisons of CS/DS content between 4 and 12 week age groups also did not reach statistical significance, except with *HAS3*-deficiency (p=0.034)), which highlights the decrease in CS/DS contents with tendon maturation in the absence of HAS3 only. At 4 weeks of age, HAS1-deficiency (Has1KO) resulted in decreased expression of *Dcn* (−3.23-fold, p=0.03), *Bgn* (−2.65-fold, p=0.004), and *Fmod* (−4.55-fold, p=0.01) relative to WT, and HAS3-deficiency (Has3KO) resulted in reduced expression of *Bgn* (−3.68-fold, p=0.001) only. These reductions in expression returned to WT levels by 12 weeks of age (p>0.05, Table 3). Notably, maturation from 4 to 12 weeks of age in WT mice significantly reduced the expression of *Bgn* (p=0.001) and *Fmod* (p=0.007). Conversely, *HAS1*-deficiency resulted in increased *Dcn* expression (p=0.009) with maturation. No age-related changes with HAS3-deficiency were observed (p>0.05, Table 3).

The Effect of HAS Deficiency on Geometric and Biomechanical Properties in Achilles Tendons

Tendon cross-sectional area (CSA) for all genotypes increased by approximately 50% (p<0.05) between 4 weeks and 12 weeks, consistent with rapid growth (Figure 5A). Tendons deficient in both HAS1 and HAS3 (Has1/3KO) showed a significant (p<0.05) difference (20% decrease) relative to age-matched WT, but only at 4 weeks (Figure 5A).

Similarly, no significant differences in stress relaxation percentage or QLV modeling coefficients were detected among genotypes, except for QLV coefficient B which showed significant differences (p<0.05), but only with *HAS3*-deficiency at 8 weeks (Figure 5B). With the exception of QLV coefficient A for WT tendons, elastic parameters A and B generally showed increases with age for each genotype, indicative of increased stiffness during low strain mechanical behavior. However, for the primary indices of viscoelastic

behavior (% relaxation and QLV coefficient C), the only significant ($p<0.05$) age-related difference observed was a decrease in % relaxation with age in *HAS3*-deficient (Has3KO) tendons (Supplemental Table 2).

Regarding differences in tissue material properties between the genotypes, significantly ($p<0.05$) increased maximum stress was noted for 8 week *HAS3*-deficient tendons (Has3KO) (Figure 5C), which was consistent with a significant increase in QLV coefficient B (Figure 5B). Interestingly, at 12 weeks of age, only HAS1-deficient tendons (Has1KO and Has1/3KO) showed significant differences in maximum stress relative to WT mice (Figure 5C). With respect to age-related differences in material properties, there was a general increase in maximum stress and elastic modulus with age for all genotypes, as expected with growth (Supplemental Table 3).

Discussion

In the current study we examined whether HAS expression and subsequent HA and CS/DS concentrations contribute to variations in morphological and biomechanical properties of un-injured tendons from WT and HAS-deficient mice at 4, 8 and 12 weeks of age. Unexpectedly, HAS-deficient mice did not display any significant differences in tendon HA contents or HAS expression compared to WT mice, at any age. Since HAS2 appears to be the predominant isoform for synthesis of high molecular weight HA in connective tissues (44), its low expression in all genotypes (WT and HAS-deficient) combined with no detectable change in the total HA concentration or stainable HA of the tendon, is consistent with the findings on post-translational control of HAS2 via protein glycosylation (45) and UDP precursor supply (46). Therefore, to further our understanding of HA regulation in tendon cell proliferation, differentiation, and ECM organization, site-specific metabolism of HAS2 within pericellular or interfibrillar tissue domains (45, 47–49), and the role of HAS1 and HAS3 (50), should be explored. Specifically, as no murine reactive antibodies to the HAS proteins exist, and knockout of the HAS2 gene is lethal (33), the use of an inducible HAS2 mutant in tissue specific promoter mouse lines (51, 52) would be of interest to delineate the age-specific role of HAS2 in tendon.

While few differences were noted structurally in the Achilles tendon for each of the three age groups and four genotypes examined, HAS1-deficiency (in the single or Has1/3 double KO) impeded the post-natal formation of the retrocalcaneal bursa. This bursa lies directly adjacent to the distal region of the Achilles, and has been implicated in the sliding motion of the retromalleolar fat pad to achieve optimal insertion of the Achilles tendon into the calcaneus during ankle flexion and extension (53). The synovial fluid of the retrocalcaneal bursa is rich in HA (3), which is evident in all HAS1-containing mice used in the current study. Additionally, HA from the retrocalcaneal bursa formed a distinct surface layer on the cartilage and peritenon surfaces. Conversely, localization of HA in the joint of the HAS1-deficient mice revealed the presence of HA-rich cell aggregates in the bursal space and a lack of surface lining associated HA, which supports a role for HAS1 in cellular activities downstream of HA synthesis, including cell survival and receptor mediated HA clearance. Although HAS1 and HAS1/3-deficiency blocked bursal formation, it did not consistently affect the biomechanical properties of the Achilles tendon. However, it should be noted that

the biomechanical testing in the current study was conducted on the tendon-calcaneus complex only, without the presence of the retrocalcaneal bursa. Thus, future studies should focus on functional characteristics of the entire limb using parameters such as gait analysis and weight bearing. Additionally, as retrocalcaneal bursa formation occurs *in-utero* (approximately 9.5 weeks in humans) (54), future studies aimed at discerning whether *Has1* deletion impedes initial formation of the bursa and/or impacts maturation during postnatal usage of the hind limbs, are warranted. In this manner, as the initial formation of the bursa has been postulated to facilitate fibrocartilage differentiation (54), studies focused on the development of a functional Achilles enthesis with knockout of *Has1* would provide novel information, given that no morphological differences were identified in the Achilles tendon itself for the current study.

It was reported that HAS1-deficient mice exhibit defective reparative responses in dermal wound-healing (55) and posttraumatic cartilage regeneration (21). In the current study, the deletion of *Has1* alone reduced the expression of *Col3a1* relative to WT particularly at 12 weeks, supporting the presence of un-organized tissue at maturation. In this regard, it may be significant that picrosirius red stained polarized light images exhibited areas of apparent disorganized collagen fibers in tendon regions of HAS1-deficient (Has1KO) mice during periods of rapid tissue remodeling, such as during growth (4 weeks old). However, these alterations in collagen organization and content did not consistently manifest as changes in biomechanical properties.

Notably, tendon CS/DS content was statistically reduced from 4 to 12 weeks of age, but only with HAS3-deficiency and borderline significant reduction was reached with HAS1& HAS3 deficiency. However, no significant differences were noted between WT and HAS-deficient genotypes between 8 and 12 week old time-points. In this context, the potential contributions of GAGs to tendon viscoelasticity have been studied using transgenic mice and GAG digestion protocols (56, 57). The dynamic modulus of Achilles tendons from skeletally mature $Bgn^{-/-}$ and $Dcn^{-/-}$ mice was reduced relative to WT, and the mutant tendons exhibited greater viscous behavior under dynamic loading (58). Whether these changes were the result of protein or GAG deficiencies was not determined. In the current study, reduced *Dcn*, and *Fmod* expression in HAS1-deficient (Has1KO) tendons, and reduced *Bgn* expression in both HAS1-deficient and HAS3-deficient (Has3KO) mice at 4 weeks of age, suggests a role for HAS(s) in tendon SLRP function during tendon growth, but probably not in maturation, as the expression patterns normalized to WT levels over time. The QLV modeling analyses in the current study revealed that there were no differences between the genotypes except for parameter B, reflective of the non-linear elastic tendon behavior under low strain.

In summary, the data presented here suggest that HA metabolism does not significantly influence the ECM structure of the tendon body, as determined by the current methodologies, but is required for maintenance of the synovial bursa. Thus, this work is relevant to the increasing realization (59, 60) that insertional Achilles tendinopathies (considered as a major subtype of Achilles disease (61) are associated with impingement of the tendon/bursa on the calcaneus, thus impairing fluid flow from the retrocalcaneal area to the tendon body and the surrounding peritenon (62). Indeed, the possible development of a

genetic model of retrocalcaneal bursal pathology in the Has1KO mouse could set a framework for studies incorporating this important component of Achilles disease. Therefore, continued studies are warranted to examine the metabolism of HA in normal maintenance of the bursa, and alterations in these pathways in the development and healing of tendon injuries and tendinopathies

Supplementary Material

Refer to Web version on PubMed Central for supplementary material.

Acknowledgements:

This work was supported by the National Institutes of Health AR63144 (VMW); Program of Excellence in Glycosciences NHLBI HL107147 (RJM); RUMC Arthritis Institute (AP), and Katz Rubschlager Endowment for OA Research (AP). The authors would like to thank Dr. Kelly Santangelo of Colorado State University for her helpful feedback during the preparation of this manuscript.

Abbreviations

Bgn	Biglycan Gene
CS	Chondroitin sulfate
CS/DS	Chondroitin/dermatan sulfate
Col1a1	Collagen Type I alpha1 gene
Col3a1	Collagen Type III alpha1 gene
CSA	Cross-Sectional Area
Dcn	Decorin gene
DS	Dermatan Sulfate
ECM	Extracellular Matrix
Fmod	Fibromodulin gene
GAG	Glycosaminoglycan
HA	Hyaluronan
HABPs	Hyaluronan Binding Proteins
Has1	Hyaluronan Synthase 1 gene
Has2	Hyaluronan Synthase 2 gene
Has3	Hyaluronan Synthase 3 gene
HAS	Hyaluronan Synthase
Has1KO	*Has1*$^{-/-}$

Has3KO	*Has3*$^{-/-}$
Has1/3KO	*Has1*$^{-/-}$, 3$^{-/-}$
QLV	Quasi-Linear Viscoelastic
PSR	Picrosirius Red
SafO	SafraninO
SLRPs	Small Leucine Rich Proteoglycans
WT	Wild-Type

References

1. Schmidt TA, Gastelum NS, Nguyen QT, et al. Boundary lubrication of articular cartilage: role of synovial fluid constituents. Arthritis and rheumatism. 2007;56(3):882–91. [PubMed: 17328061]
2. Culav EM, Clark CH, Merrilees MJ. Connective tissues: matrix composition and its relevance to physical therapy. Phys Ther. 1999;79(3):308–19. [PubMed: 10078774]
3. Canoso JJ, Stack MT, Brandt KD. Hyaluronic acid content of deep and subcutaneous bursae of man. Ann Rheum Dis. 1983;42(2):171–5. [PubMed: 6847262]
4. Cowman MK, Schmidt TA, Raghavan P, Stecco A. Viscoelastic Properties of Hyaluronan in Physiological Conditions. F1000Res 2015;4:622. [PubMed: 26594344]
5. Dicker KT, Gurski LA, Pradhan-Bhatt S, et al. Hyaluronan: a simple polysaccharide with diverse biological functions. Acta biomaterialia. 2014;10(4):1558–70. [PubMed: 24361428]
6. Day AJ. The structure and regulation of hyaluronan-binding proteins. Biochem Soc Trans. 1999;27(2):115–21. [PubMed: 10093718]
7. Kielty CM, Hopkinson I, Grant ME. Collagen: the collagen family, structure, assembly, and organization in the extracellular matix In: P.M. R, B.S. S, editors. Connective Tissue and Its Heritable Disorders: Molecular, Genetic, and Medical Aspects. New York, NY: Wiley-Liss; 1993 p. 103–47.
8. Wisniewski HG, Burgess WH, Oppenheim JD, Vilcek J. TSG-6, an arthritis-associated hyaluronan binding protein, forms a stable complex with the serum protein inter-alpha-inhibitor. Biochemistry. 1994;33(23):7423–9. [PubMed: 7516184]
9. Itano N, Kimata K. Mammalian hyaluronan synthases. IUBMB Life. 2002;54(4):195–9. [PubMed: 12512858]
10. Siiskonen H, Oikari S, Pasonen-Seppanen S, Rilla K. Hyaluronan synthase 1: a mysterious enzyme with unexpected functions. Front Immunol. 2015;6:43. [PubMed: 25699059]
11. Sugi Y, Yamamura H, Okagawa H, Markwald RR. Bone morphogenetic protein-2 can mediate myocardial regulation of atrioventricular cushion mesenchymal cell formation in mice. Dev Biol. 2004;269(2):505–18. [PubMed: 15110716]
12. Ma L, Lu MF, Schwartz RJ, Martin JF. Bmp2 is essential for cardiac cushion epithelial-mesenchymal transition and myocardial patterning. Development. 2005;132(24):5601–11. [PubMed: 16314491]
13. Lagendijk AK, Szabo A, Merks RM, Bakkers J. Hyaluronan: a critical regulator of endothelial-to-mesenchymal transition during cardiac valve formation. Trends Cardiovasc Med. 2013;23(5):135–42. [PubMed: 23295082]
14. Vigetti D, Karousou E, Viola M, et al. Hyaluronan: biosynthesis and signaling. Biochimica et biophysica acta. 2014;1840(8):2452–9. [PubMed: 24513306]
15. Rilla K, Oikari S, Jokela TA, et al. Hyaluronan synthase 1 (HAS1) requires higher cellular UDP-GlcNAc concentration than HAS2 and HAS3. The Journal of biological chemistry. 2013;288(8):5973–83. [PubMed: 23303191]

16. Yang G, Jiang B, Cai W, et al. Hyaluronan and hyaluronan synthases expression and localization in embryonic mouse molars. J Mol Histol. 2016;47(4):413–20. [PubMed: 27318667]
17. Kim JD, Kim HJ, Koun S, et al. Zebrafish Crip2 plays a critical role in atrioventricular valve development by downregulating the expression of ECM genes in the endocardial cushion. Molecules and cells. 2014;37(5):406–11. [PubMed: 24823359]
18. Ghatak S, Misra S, Norris RA, et al. Periostin induces intracellular cross-talk between kinases and hyaluronan in atrioventricular valvulogenesis. The Journal of biological chemistry. 2014;289(12): 8545–61. [PubMed: 24469446]
19. Veerkamp J, Rudolph F, Cseresnyes Z, et al. Unilateral dampening of Bmp activity by nodal generates cardiac left-right asymmetry. Developmental cell. 2013;24(6):660–7. [PubMed: 23499359]
20. Tien JY, Spicer AP. Three vertebrate hyaluronan synthases are expressed during mouse development in distinct spatial and temporal patterns. Developmental dynamics : an official publication of the American Association of Anatomists. 2005;233(1):130–41. [PubMed: 15765504]
21. Chan DD, Xiao WF, Li J, et al. Deficiency of hyaluronan synthase 1 (Has1) results in chronic joint inflammation and widespread intra-articular fibrosis in a murine model of knee joint cartilage damage. Osteoarthritis and Cartilage. 2015;23(11):1879–89. [PubMed: 26521733]
22. Chan DD, Li J, Luo W, et al. Pirfenidone reduces subchondral bone loss and fibrosis after murine knee cartilage injury. Journal of orthopaedic research : official publication of the Orthopaedic Research Society. 2017.
23. Scott JE, Orford CR, Hughes EW. Proteoglycan-collagen arrangements in developing rat tail tendon. An electron microscopical and biochemical investigation. The Biochemical journal. 1981;195(3):573–81. [PubMed: 6459082]
24. Connizzo BK, Sarver JJ, Birk DE, et al. Effect of age and proteoglycan deficiency on collagen fiber re-alignment and mechanical properties in mouse supraspinatus tendon. J Biomech Eng. 2013;135(2):021019. [PubMed: 23445064]
25. Dunkman AA, Buckley MR, Mienaltowski MJ, et al. Decorin expression is important for age-related changes in tendon structure and mechanical properties. Matrix biology : journal of the International Society for Matrix Biology. 2013;32(1):3–13. [PubMed: 23178232]
26. Chen S, Birk DE. The regulatory roles of small leucine-rich proteoglycans in extracellular matrix assembly. The FEBS journal. 2013;280(10):2120–37. [PubMed: 23331954]
27. Zhang G, Ezura Y, Chervoneva I, et al. Decorin regulates assembly of collagen fibrils and acquisition of biomechanical properties during tendon development. Journal of cellular biochemistry. 2006;98(6):1436–49. [PubMed: 16518859]
28. Jepsen KJ, Wu F, Peragallo JH, et al. A syndrome of joint laxity and impaired tendon integrity in lumican- and fibromodulin-deficient mice. The Journal of biological chemistry. 2002;277(38): 35532–40. [PubMed: 12089156]
29. Svensson L, Aszodi A, Reinholt FP, et al. Fibromodulin-null mice have abnormal collagen fibrils, tissue organization, and altered lumican deposition in tendon. The Journal of biological chemistry. 1999;274(14):9636–47. [PubMed: 10092650]
30. Ameye L, Aria D, Jepsen K, et al. Abnormal collagen fibrils in tendons of biglycan/fibromodulin-deficient mice lead to gait impairment, ectopic ossification, and osteoarthritis. FASEB journal : official publication of the Federation of American Societies for Experimental Biology. 2002;16(7): 673–80. [PubMed: 11978731]
31. Kiene LS, Homann S, Suvorava T, et al. Deletion of Hyaluronan Synthase 3 Inhibits Neointimal Hyperplasia in Mice. Arterioscler Thromb Vasc Biol. 2016;36(2):e9–16. [PubMed: 26586662]
32. Kessler SP, Obery DR, de la Motte C. Hyaluronan Synthase 3 Null Mice Exhibit Decreased Intestinal Inflammation and Tissue Damage in the DSS-Induced Colitis Model. Int J Cell Biol. 2015;2015:745237. [PubMed: 26448758]
33. Camenisch TD, Spicer AP, Brehm-Gibson T, et al. Disruption of hyaluronan synthase-2 abrogates normal cardiac morphogenesis and hyaluronan-mediated transformation of epithelium to mesenchyme. The Journal of clinical investigation. 2000;106(3):349–60. [PubMed: 10930438]

34. Trella KJ, Li J, Stylianou E, et al. Genome-wide analysis identifies differential promoter methylation of Leprel2, Foxf1, Mmp25, Igfbp6 and Peg12 in murine tendinopathy. Journal of orthopaedic research : official publication of the Orthopaedic Research Society. 2017;35(5):947–55.
35. Bell R, Li J, Gorski DJ, et al. Controlled treadmill exercise eliminates chondroid deposits and restores tensile properties in a new murine tendinopathy model. Journal of biomechanics. 2013;46(3):498–505. [PubMed: 23159096]
36. Dayan D, Hiss Y, Hirshberg A, et al. Are the polarization colors of picrosirius red-stained collagen determined only by the diameter of the fibers? Histochemistry. 1989;93(1):27–9. [PubMed: 2482274]
37. Junqueira LC, Bignolas G, Brentani RR. Picrosirius staining plus polarization microscopy, a specific method for collagen detection in tissue sections. Histochem J. 1979;11(4):447–55. [PubMed: 91593]
38. Wang VM, Bell RM, Thakore R, et al. Murine tendon function is adversely affected by aggrecan accumulation due to the knockout of ADAMTS5. Journal of orthopaedic research : official publication of the Orthopaedic Research Society. 2012;30(4):620–6.
39. Calabro A, Midura R, Wang A, et al. Fluorophore-assisted carbohydrate electrophoresis (FACE) of glycosaminoglycans. Osteoarthritis and cartilage / OARS, Osteoarthritis Research Society. 2001;9 Suppl A:S16–22.
40. Calabro A, Benavides M, Tammi M, et al. Microanalysis of enzyme digests of hyaluronan and chondroitin/dermatan sulfate by fluorophore-assisted carbohydrate electrophoresis (FACE). Glycobiology. 2000;10(3):273–81. [PubMed: 10704526]
41. Funk JR, Hall GW, Crandall JR, Pilkey WD. Linear and quasi-linear viscoelastic characterization of ankle ligaments. J Biomech Eng. 2000;122(1):15–22. [PubMed: 10790825]
42. Huang CY, Wang VM, Flatow EL, Mow VC. Temperature-dependent viscoelastic properties of the human supraspinatus tendon. Journal of biomechanics. 2009;42(4):546–9. [PubMed: 19159888]
43. Abramowitch SD, Woo SL, Clineff TD, Debski RE. An evaluation of the quasi-linear viscoelastic properties of the healing medial collateral ligament in a goat model. Annals of biomedical engineering. 2004;32(3):329–35. [PubMed: 15098537]
44. Jokela T, Karna R, Rauhala L, et al. Human Keratinocytes Respond to Extracellular UTP by Induction of Hyaluronan Synthase 2 Expression and Increased Hyaluronan Synthesis. The Journal of biological chemistry. 2017;292(12):4861–72. [PubMed: 28188289]
45. Vigetti D, Passi A. Hyaluronan synthases posttranslational regulation in cancer. Adv Cancer Res. 2014;123:95–119. [PubMed: 25081527]
46. Hascall VC, Wang A, Tammi M, et al. The dynamic metabolism of hyaluronan regulates the cytosolic concentration of UDP-GlcNAc. Matrix biology : journal of the International Society for Matrix Biology. 2014;35:14–7. [PubMed: 24486448]
47. Tiainen S, Oikari S, Tammi M, et al. High extent of O-GlcNAcylation in breast cancer cells correlates with the levels of HAS enzymes, accumulation of hyaluronan, and poor outcome. Breast Cancer Res Treat. 2016;160(2):237–47. [PubMed: 27683279]
48. Jokela TA, Karna R, Makkonen KM, et al. Extracellular UDP-glucose activates P2Y14 Receptor and Induces Signal Transducer and Activator of Transcription 3 (STAT3) Tyr705 phosphorylation and binding to hyaluronan synthase 2 (HAS2) promoter, stimulating hyaluronan synthesis of keratinocytes. The Journal of biological chemistry. 2014;289(26):18569–81. [PubMed: 24847057]
49. Vigetti D, Deleonibus S, Moretto P, et al. Role of UDP-N-acetylglucosamine (GlcNAc) and O-GlcNAcylation of hyaluronan synthase 2 in the control of chondroitin sulfate and hyaluronan synthesis. The Journal of biological chemistry. 2012;287(42):35544–55. [PubMed: 22887999]
50. Koistinen V, Karna R, Koistinen A, et al. Cell protrusions induced by hyaluronan synthase 3 (HAS3) resemble mesothelial microvilli and share cytoskeletal features of filopodia. Exp Cell Res. 2015;337(2):179–91. [PubMed: 26162854]
51. Walker JKL, Theriot BS, Ghio M, et al. Targeted HAS2 Expression Lessens Airway Responsiveness in Chronic Murine Allergic Airway Disease. Am J Respir Cell Mol Biol. 2017;57(6):702–10. [PubMed: 28787175]

52. Chien C, Pryce B, Tufa SF, et al. Optimizing a 3D model system for molecular manipulation of tenogenesis. Connect Tissue Res. 2017:1–14.

53. Canoso JJ, Liu N, Traill MR, Runge VM. Physiology of the retrocalcaneal bursa. Ann Rheum Dis. 1988;47(11):910–2. [PubMed: 3207374]

54. Shaw HM, Vazquez OT, McGonagle D, et al. Development of the human Achilles tendon enthesis organ. J Anat. 2008;213(6):718–24. [PubMed: 19094187]

55. Mack JA, Feldman RJ, Itano N, et al. Enhanced inflammation and accelerated wound closure following tetraphorbol ester application or full-thickness wounding in mice lacking hyaluronan synthases Has1 and Has3. The Journal of investigative dermatology. 2012;132(1):198–207. [PubMed: 21850020]

56. Dourte LM, Pathmanathan L, Mienaltowski MJ, et al. Mechanical, compositional, and structural properties of the mouse patellar tendon with changes in biglycan gene expression. Journal of orthopaedic research : official publication of the Orthopaedic Research Society. 2013;31(9):1430–7.

57. Robinson PS, Huang TF, Kazam E, et al. Influence of decorin and biglycan on mechanical properties of multiple tendons in knockout mice. J Biomech Eng. 2005;127(1):181–5. [PubMed: 15868800]

58. Gordon JA, Freedman BR, Zuskov A, et al. Achilles tendons from decorin- and biglycan-null mouse models have inferior mechanical and structural properties predicted by an image-based empirical damage model. Journal of biomechanics. 2015;48(10):2110–5. [PubMed: 25888014]

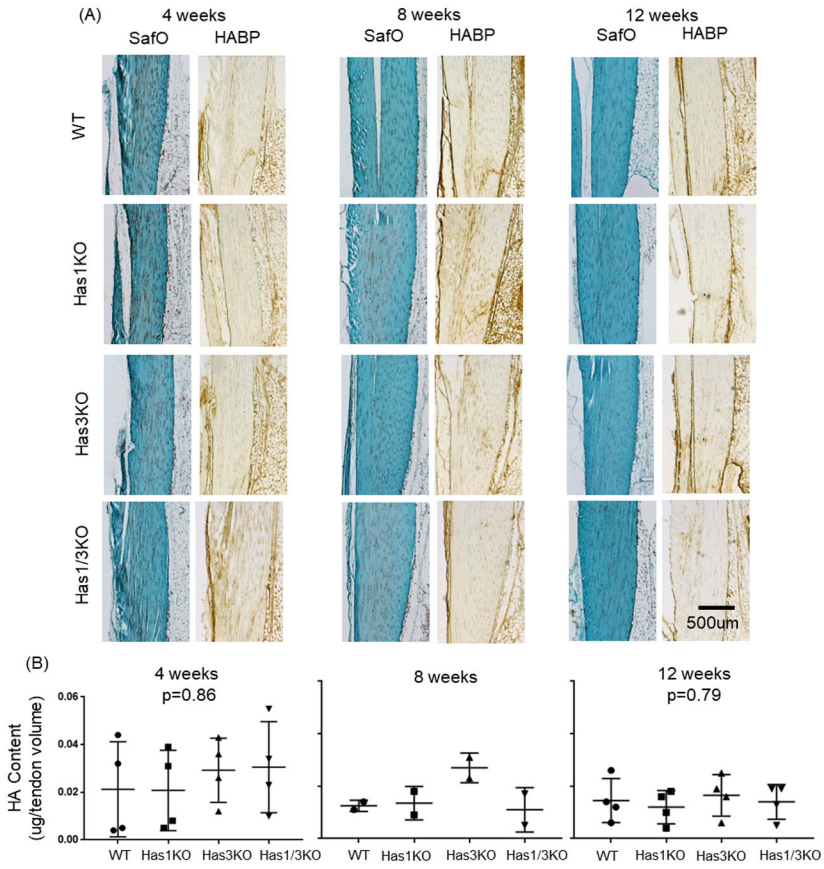

Figure 1:

(A) SafraninO and hyaluronan binding protein (HABP) staining of the tendon body from all four genotypes at 4, 8, and 12 weeks of age. (B) HA contents (determined through FACE) in Achilles tendons from all four genotypes and all three ages. Number of tendon pools assayed for HA contents are provided in Table 1. Data points represent individual tendons, with box/whiskers denoting average +/− STD; p-values between age-matched genotypes listed for 4 and 12 weeks only; no significance detected between genotyped matched 4, or 12 week olds.

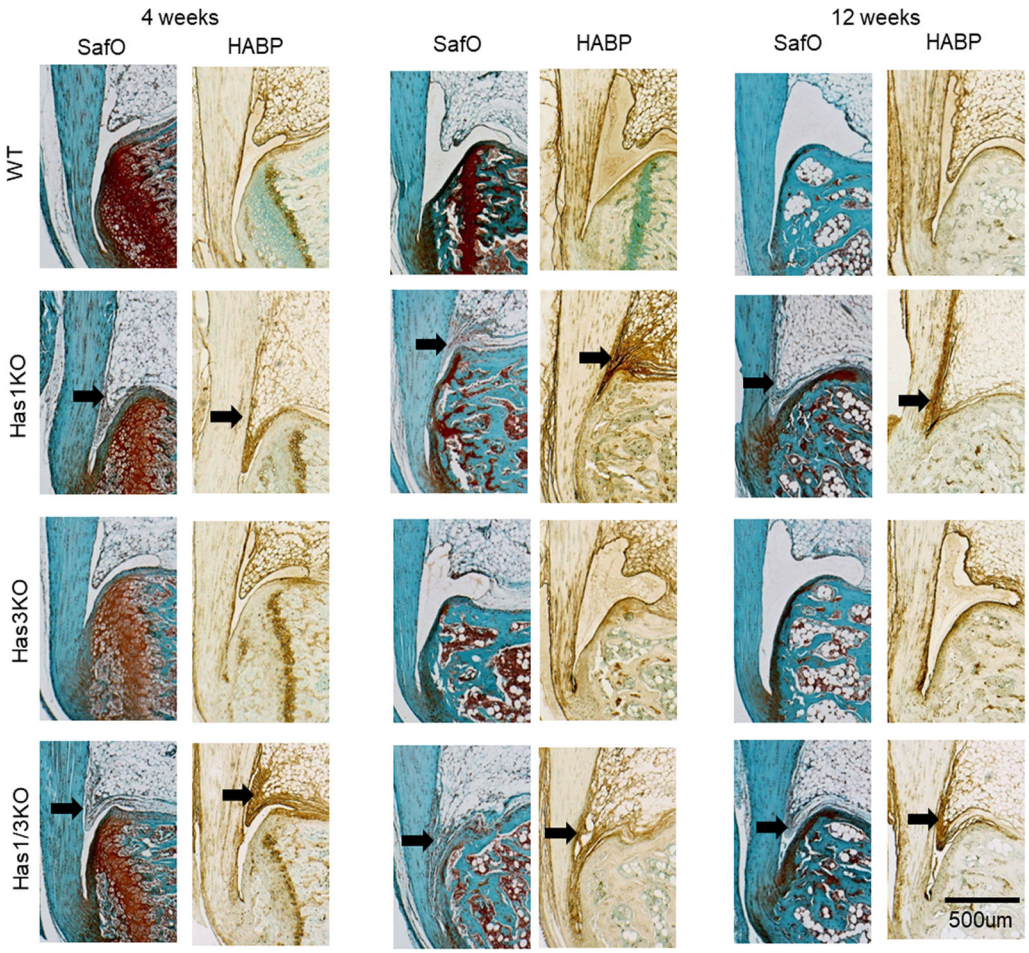

Figure 2:

SafraninO (SafO) and hyaluronan binding (HABP) protein staining of the Achilles-calcaneus insertion from all four genotypes at 4, 8, and 12 weeks of age. Black arrows denote absence of the synovial bursa adjacent to the Achilles tendon.

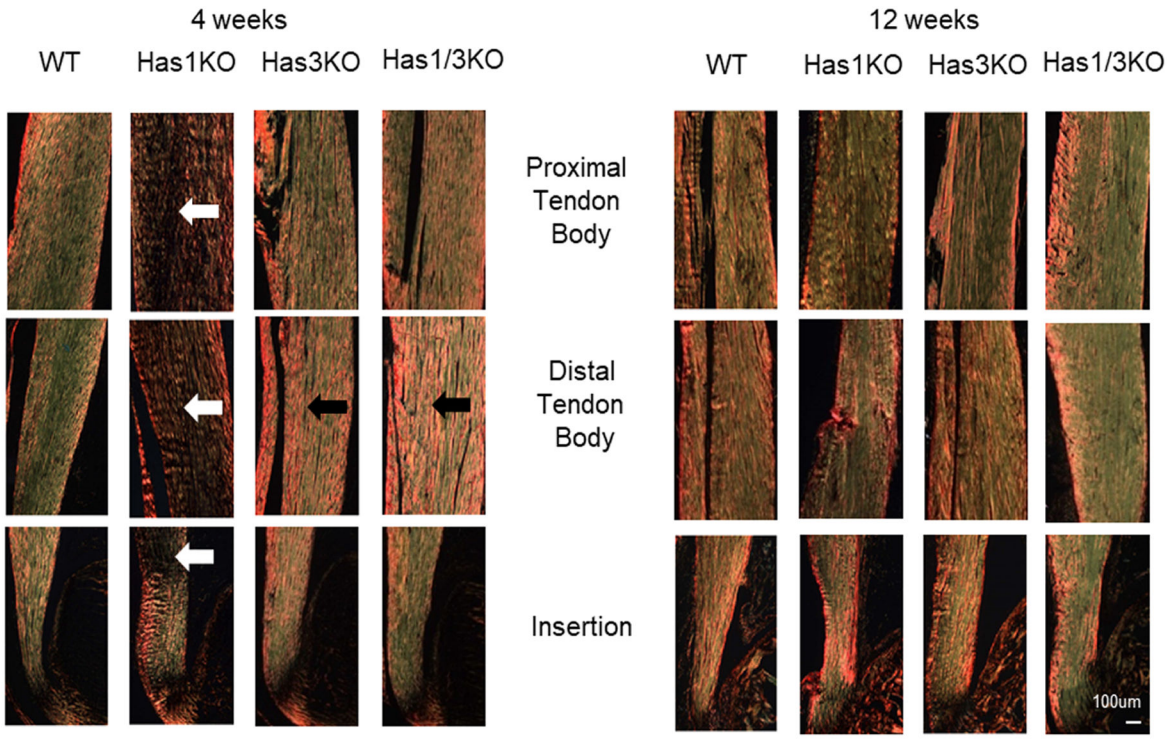

Figure 3:

Representative polarized light microscopy images of picrosirius red-stained Achilles tendon sections from all four genotypes at 4 and 12 weeks of age. White arrows denote areas of un-organized collagen, while black arrows denote densely packed fibers.

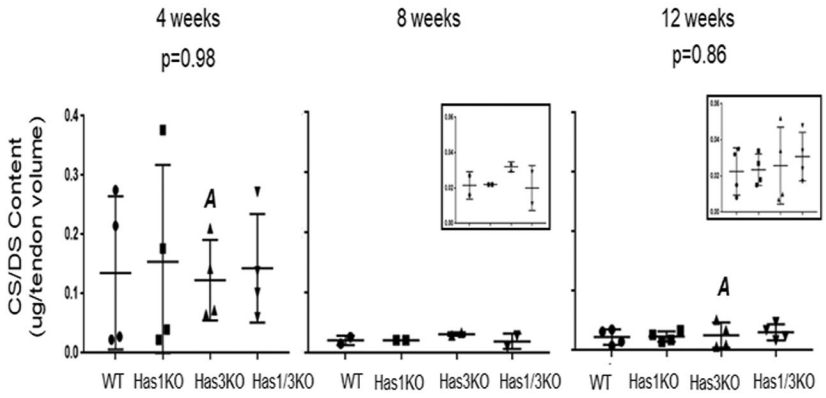

Figure 4:

CS/DS contents (determined through FACE) in Achilles tendons from all four genotypes and all three ages. Number of tendon pools assayed for CS/DS contents can be seen in Table1. Data points represent individual tendon pools, with box/whiskers denoting average +/− STD; p-values between age-matched genotypes listed for 4 and 12 weeks only; no significance detected between genotyped matched 4 or 12 week olds except for Has3KO (12 week relative to 4 week; p=0.034, marked with matching letters).

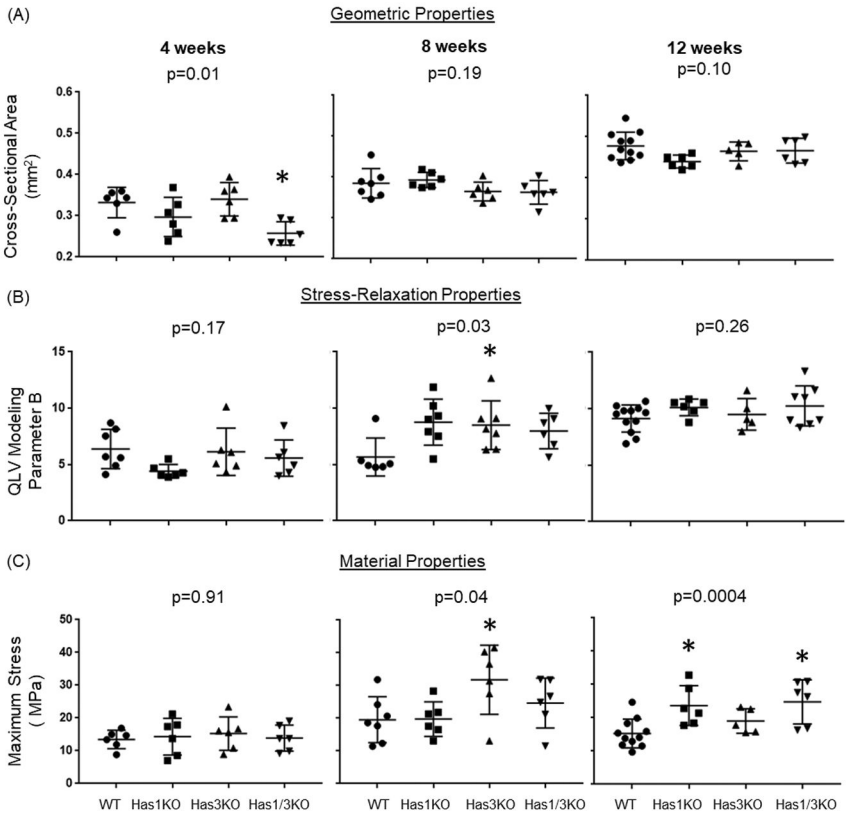

Figure 5:

Geometric, stress relaxation, and material properties of Achilles tendons from all four genotypes at 4, 8, and 12 weeks of age. Data points represent individual tendons, with box/whiskers denoting average +/− STD. p-values between age-matched genotypes listed. Only parameters with significant differences between genotypes at each age are shown (*p<0.05). All parameters measured during testing are provided inSupplemental Table 2 and 3 for stress relaxation, and geometric/material properties, respectively.

Table 1:

Experimental Groups and Outcomes

Age (weeks)	Genotype	Histology/IHC/PSR[1]	Biomechanics[1]	Gene Expression[2]	FACE[2]
4	WT	n=3	n=6	n=3 (10,16,16)	n=4 (6,6,8,8)
	HaslKO	n=3	n=6	n=3 (20,16,16)	n=4 (6,6,8,8)
	Has3KO	n=3	n=6	n=3 (18,14,14)	n=4 (5,5,8,8)
	Has1/3KO	n=2	n=6	n=l (20)	n=4 (6,6,8,8)
8	WT	n=3	n=7	n=l (20)	n=2 (6,6)
	HaslKO	n=3	n=6	n=l (18)	n=2 (6,6)
	Has3KO	n=3	n=6	n=l (18)	n=2 (5,5)
	Has1/3KO	n=3	n=6	n=l (16)	n=2 (5,5)
12	WT	n=4	n=ll	n=3 (20,20,20)	n=4 (6,6,8,8)
	HaslKO	n=5	n=6	n=3 (24,20,20)	n=4 (8,8,8,8)
	Has3KO	n=5	n=5	n=3 (18,15,15)	n=4 (7,7,8,8)
	Has1/3KO	n=5	n=6	n=l (22)	n=4 (6,6,8,8)

[1] Number of limbs

[2] Tissue pools with the number of tendons per pool listed in parenthesis (both legs utilized)

Table 2:

Apparent mRNA Abundance for Hyaluronan Synthase1,2 and 3 genes in WT and HasKO tendons at 4, 8, and 12 weeks of age

Gene	Age	WT[1]	Has1KO[1]		Has3KO[1]		Has1/3KO[2]	
	(weeks)	Abundance[3]	Abundance[3]	Fold[4]	Abundance[3]	Fold[4]	Abundance[3]	Fold[4]
Has1	4	3.35 (±1.43)	ND	-	3.10 (±3.25)	−1.04 (±2.80)	ND	-
	8	2.98	ND	-	1.58	−1.89	ND	-
	12	3.02 (±0.97)	ND	-	3.95 (±2.41)	1.36 (±0.83)	ND	-
Has2	4	0.42 (±0.15)	0.45 (±0.40)	−0.60 (±2.51)	0.16 (±0.08)	−3.21 (±2.08)	0.09	−4.78
	8	0.16	0.08	−1.97	0.11	−1.46	0.09	−1.71
	12	0.29 (±0.18)	0.45 (±0.54)	−0.13 (±3.95)	0.26 (±0.13)	0.12 (±2.09)	0.22	−1.13
Has3	4	ND	ND	-	ND	-	ND	-
	8	ND	ND	-	ND	-	ND	-
	12	ND	ND	-	ND	-	ND	-

[1] Assays were performed on n=3 individual pools of tendons for 4 and 12 week time points, with average values ± standard deviations presented. For the 8 week time point only one pool was assayed. See Table 1 for details.

[2] Assays were performed on one pool of tendons for all three time points. See Table 1 for details

[3] Data were calculated as apparent mRNA abundance relative to *Gapdh*. See Methods for details.

[4] Fold change in *Has*-deficient genotypes relative to WT. See Methods for details

Statistical evaluation showed no significant differences in apparent mRNA abundance for age-matched genotype comparisons and genotype-matched age comparisons ($p>0.05$).

ND=Not detectable (Ct values >34 cycles)

Table 3:

Apparent mRNA abundance of extracellular matrix genes in WT and HasKO tendons at 4, 8, and 12 weeks of age

Gene	Age	WT[1]		Has1KO[1]			Has3KO[1]			Has1/3KO[2]	
	(weeks)	Abundance[3]	Sig[5,6]	Abundance[3]	Fold[4]	Sig[5,6]	Abundance[3]	Fol[4]	Sig[5,6]	Abundance[3]	Fold[4]
Collal	4	36004 (±16423)	AAA	10785(±4484)	−3.69 (±2.01)	E	14637(±13743)	−3.77 (±2.37)		11705	−2.89
	8	2383		1417	−1.68		9363	3.93		3688	1.55
	12	3699 (±958)	AAA	2346 (±654.2)	−1.63 (±0.48)	E	4206 (±1898)	−0.19 (±1.70)		2591	−1.39
Col3al	4	1248(±930)	B	501.5 (±421.3)	−3.21 (±2.27)	FF	763.5 (±572.1)	−1.11 (±2.17)	H	202.8	−5.05
	8	90.43		33.73	−2.68		133.5	1.48		58.8	−1.54
	12	173.8 (±24.59)	B	18.27 (±11.12)	−13.54 (±10.54)	FF ***	152.1 (±79.03)	−0.630 (±1.77)	H	193.4	1.12
Dcn	4	5445(±2481)		1637 (±391.0)	−3.23 (±0.69)	GG *	5576 (±2780)	−0.29 (±1.74)		2371.8	−2.15
	8	2864		2459	−1.16		4763	1.66		2207	−1.3
	12	7927 (±2521)		133209(±9664)	1.06 (±2.16)	GG	4788 (±344.2)	−1.61 (±0.11)		3456	−2.22
Bgn	4	1565 (±220.4)	CCC	604.9 (±123.2)	−2.65 (±0.57)	***	445.0 (±131.5)	−3.68 (±0.98)	***	438.9	−3.54
	8	183.3		177.5	−1.07		246.2	1.3		164.9	−1.15
	12	343.0 (±88.16)	CCC	545.1 (±256.1)	0.94 (±1.93)		333.4 (±103.7)	0.26 (±1.57)		377.1	1.13
Fmod	4	4314 (±2319)	DD	880.5 (±131.6)	−4.55 (±0.70)	**	2096(±1014)	−2.18 (±0.95)		1268	−3.11
	8	573.2		399.4	−1.43		1087	1.9		671.3	1.17
	12	666.5 (±247.4)	DD	913.3 (±187.5)	1.43 (±0.29)		1138 (±184.3)	1.78 (±0.29)		772.2	1.21

[1] Assays were performed on n= 3 individual pools of tendons for 4 and 12 week time points, with average values ± standard deviations presented. For the 8 week time point only one pool was assayed. See Table 1 for details.

[2] Assays were performed on one pool of tendons for all three time points. See Table 1 for details

[3] Data were calculated as apparent mRNA abundance relative to *Gapdh*. See Methods for details.

[4] Fold change in Has-*deficient* genotypes relative to WT. See Methods for details

[5] Asterisks denote significant differences in expression between *Has*-deficient genotypes relative to age-matched WT (statistics performed on 4 and 12 week, Has1KO and Has3KO groups only;

* p<0.05,

** p<0.01,

*** p<0.005).

[6] Matching letters (A-F) denote significant differences in expression between genotype-matched 4 and 12 week olds (example: A; $p<0.05$, AA; $p<0.01$, AAA; $p<0.005$).